RSC Advances

RSC Publishing

PAPER

View Article Online
View Journal | View Issue

Cite this: *RSC Adv.*, 2013, **3**, 26297

A micromachined impedance biosensor for accurate and rapid detection of *E. coli* O157:H7

Shibajyoti Ghosh Dastider,[a] Syed Barizuddin,[b] Majed Dweik[b] and Mahmoud Almasri*[a]

An impedance biosensor based on interdigitated electrode (IDE) arrays was designed, fabricated and tested for detection of *Escherichia coli* O157:H7. The device consists of two sets of gold IDE arrays embedded in a SU8-PDMS microchannel. The first set of electrodes uses positive dielectrophoresis (p-DEP) force to focus and concentrate the *E. coli* into the centre of the microchannel, and direct it towards the detection zone microchannel which has dimensions of a third of the first channel. The bulk fluid keeps flowing toward the outer channel into the waste outlets. The second sets of electrodes are located in the centre channel and are used for impedimetric detection of the *E. coli*. A combination of standard photolithography, wet etching and plasma treatment techniques were used to fabricate the biosensor. The *E. coli* cells in the test solution were focused into the centre of the channel when an excitation signal of 5 V_{p-p} at 5.6 MHz was applied across the electrode arrays. Before injecting the *E. coli* cells, polyclonal anti-*E. coli* antibodies were non-specifically immobilized on the sensing electrode array. This ensures specific detection of *E. coli* O157:H7 bacterial cells. As the concentrated *E. coli* cells (antigen) reach the sensing electrode array, they bind to the immobilized antibody sites. This antigen–antibody binding causes a change in the impedance, which is measured using an impedance analyzer. The device performance was tested by measuring the impedance, between 100 Hz and 1 MHz frequency, before and after applying p-DEP on the focusing electrode array, and after applying p-DEP on both the focusing and sensing electrodes. The result shows clearly that the use of p-DEP on the focusing IDE array significantly increased the measurement sensitivity with the lower detection limit being 3×10^2 CFU mL^{-1}. In addition, the use of p-DEP on both electrode arrays increased the measurement sensitivity by a factor of 2.9 to 4.5 times depending on the concentration.

Received 28th August 2013
Accepted 23rd October 2013

DOI: 10.1039/c3ra44724c

www.rsc.org/advances

Introduction

The Centers for Disease Control and Prevention estimates that foodborne diseases cause illness in an estimated 48 million people every year, causing 128 000 hospitalizations and 3000 fatalities.[1] Just in the last six months of 2012, there were sixteen food related outbreaks in the United States.[2] These outbreaks were caused by transmission of pathogens to humans *via* contaminated fruit, vegetables, meat, drinking water, milk, poultry and eggs. CDC reports that *E. coli* O157:H7, various strains of Salmonella, *Listeria monocytogenes* were reasons for food contamination.[3] Pathogens also have the potential to cause major economic losses due to the product recalls and medical costs associated with illnesses. It is noted that the cost related to foodborne illness in the US annually is estimated at $77 billion.[4] Therefore, it is of great importance to develop novel and advanced methods for more efficient detection of foodborne pathogenic bacteria. One of the most harmful pathogenic strains of *E. coli* in North America is *E. coli* O157:H7. It produces Shiga toxin that damages the intestine lining, causes anemia, stomach cramps and bloody diarrhea. Sometimes, it causes serious complications including hemolytic uremic syndrome (HUS) and thrombotic thrombocytopenic purpura (TTP).[5–8]

Conventional methods used to detect and identify pathogenic bacteria in food are reliable for ensuring food safety. They have been used for many years as the official food screening procedure established by Food and Drug Administration (FDA). However, these methods are time consuming and require 5-7 days to get conclusive results. Viable alternatives are needed to efficiently monitor food quality rapidly and provide real time response to possible risks. By the time the bacteria are detected, the product could already be sold and consumed.[9] The slow response of the current detection methods has prompted numerous groups in the last decade to develop other techniques to reduce the detection time. Polymerase Chain Reaction (PCR)

[a]*Department of Electrical and Computer Engineering, University of Missouri, 233 Engineering Building West, Columbia, MO 65211, USA. E-mail: almasrim@missouri.edu; Fax: +1-(573)-882-0397; Tel: +1-(573)-882-0813*

[b]*Department of Co-operative research, Lincoln University, Jefferson City, MO 6510, USA*

and Enzyme Linked Immunosorbent Assay (ELISA), for example, have reduced the assay time to 4–6 h and 10–24 h, respectively, with detection limits between 10^1–10^6 colony forming units (CFU) mL. Both techniques, however, have limitations that preclude their widespread implementation. These limitations include their failure to distinguish spore viability.[10–14] In the past several years, various bacteria detection biosensors have been developed with improved response time, sensitivity and reliability; with some assays requiring around 2 h under ideal conditions with a sensitivity of 10^3–10^4 CFU mL^{-1}.[15,16] Although these devices have resulted in good performance, other key issues need to be considered in order to develop rapid (real time) methods to detect pathogens. These include sample volume, cost and measurement of a single cell or small number of cells. As a result, several groups have developed miniaturized impedance biosensors with a reduced sample volume. This has resulted in high detection sensitivity, low contamination during bacterial growth, and faster detection of a small number of cells.[17–22] Currently, many groups are actively investigating the detection of pathogens using various biosensing techniques.[23–43]

The objective of this paper is to develop a Microelectromechanical system (MEMS) impedance biosensor capable of rapid detection and accurate identification of *E.coli* O157:H7. We report the detection of *E. coli* cells with a concentration range from 3×10^5–3×10^2 CFU mL^{-1} using two set of interdigitated electrode array. The first uses p-DEP to focus and concentrate the cell into the centre of the channel, while the second set is functionalized with the *E. coli* specific antibody to immobilize the bacteria for impedimetric detection. The change in impedance due to antigen–antibody binding is detected using an impedance analyzer. The main advantage of antibodies as the bio-recognition elements is their sensitivity and selectivity to target cells. The detection processes require no enrichment steps, minimal sample processing and hence the detection time of under 3 hours. Food suppliers and food packaging companies can perform real time monitoring of food products and provide healthy and safe products to local and global markets, while at the same time checking the spread of disease and preventing economic losses due to medical costs and product recalls.

Theoretical background

Dielectrophoresis (DEP) is defined as the translational motion of a dielectric particle or biological cell in a suspending medium under the influence of a non-uniform AC E-field.[44] This non-uniform E-field induces a net force in a dielectric particle or cell directed either to a region of maximum or minimum E-field strength. The driving force direction is determined by two factors: permittivity of the particle compared with that of the medium surrounding the particle, and the frequency of the applied E-field. For this device positive DEP is used to attract the cells towards the electrodes and laterally position them. By varying the magnitude and frequency of the applied signal viable target cells are attracted towards the electrodes, whereas non-target particles do not. The DEP force applied on the cells can be simplified as:

$$\vec{F}_{\mathrm{DEP}} = 2\pi\varepsilon_{\mathrm{m}} r^3 \nabla E^2 \mathrm{Re}[K(\omega)]$$

where r is the radius of the cell, ε_{m} is the medium's permittivity, and E is the electrical field. K is the Clausius–Mossotti factor. Viable *E. coli* cells are attracted towards the electrodes by adjusting the Clausius–Mossotti factor K, which can be altered by varying the frequency of the applied signal. As the viable and non-viable cells are different in composition the Clausius–Mossotti factors are different. The difference in the Clausius–Mossotti factors will result in difference in reaction to the electric field. The viable target cells are attracted towards the electrode, whereas the non-target are not, which could be used for sorting and separation of target cells.

When cells are flowing in the channel they not only experience DEP force, but also hydrodynamic force.[45] For a non-turbulent flow, where the Reynolds number is much smaller than 1 ($\mathrm{Re} \ll 1$) the hydrodynamic drag force on a moving object is linearly proportional to the object's velocity through the fluid. Hydrodynamic force acts to oppose the motion and can be described as being an energy-dissipating or frictional force. If the relative velocity between the cell and the flow is $\vec{v}$, fluid viscosity is η, for a cell with radius r this force is given by:

$$\vec{F}_{\mathrm{drag}} \approx \eta r \vec{v}$$

The ratio of the drag force to the velocity is $\frac{\vec{F}_{\mathrm{drag}}}{\vec{v}} = k_{\mathrm{drag}}$ called the drag coefficient, and is roughly equivalent to the product of viscosity and longest dimension of the cell. For a spherical particle such as cell which has a radius r, the drag coefficient is $k_{\mathrm{drag}} = 6\pi\eta r$. So, the drag force can be given by:

$$\vec{F}_{\mathrm{drag}} = 6\pi\eta r \vec{v}$$

In absence of flow, cells will get attracted towards the electrode and stay there. Therefore, to sort and separate viable cells and to move them towards the detection electrode array, a flow is required. The flow works in conjunction with the DEP and generates enough hydrodynamic force to concentrate the viable bacteria cells towards the center of the microchannel. At equilibrium, the hydrodynamic and DEP forces are equal, which gives us the minimum velocity required to move the cells towards the center channel.

$$\vec{v}_{\mathrm{min}} < \frac{\varepsilon_{\mathrm{m}} r^2}{3\eta} \mathrm{Re}[K] \frac{\partial E^2}{\partial x}$$

Thus successful separation and sorting is greatly dependent on the flow rate of the fluid inside the microchannel. Also higher flow rates can be accommodated as the length of the electrode array and number of the electrodes within the array is increased. Hydrodynamic drag force in conjunction with the p-DEP force creates a streamlined cell flow, through the center of the narrow channel towards the detection electrode array. The *E. coli* cells are recognized and captured on the detection electrode array using anti-*E. coli* antibody.

Material and methods

Biosensor design

Interdigitated microelectrode (IDE) arrays that incorporate cell separation and impedance measurement principles to facilitate low level detection of *E. coli* O157:H7 was fabricated and tested. The device consisted of two set of gold IDE array embedded in a SU-8 microchannel (Fig. 1). The focusing region consists of 100 pairs of electrodes with a channel width of 300 μm while the detection region had 25 pairs of electrodes with a channel width of 100 μm. The electrode length, width and spacing was 300 μm, 15 μm and 10 μm, respectively. The height of the channel was 25 μm. The first IDE array was designed to focus the targeted *E. coli* O157:H7 cells using p-DEP and direct them towards the center channel which has dimensions of a third of the first channel with a micro liter volume. The bulk fluid flows toward the outer channel into the waste outlets. Following the focusing region in the channels, is the detection region. The detection IDE array was functionalized using specific anti-*E. coli* specific antibodies to target the *E. coli* cells on the electrode surface. The *E. coli* samples were tested by flowing them through the microchannel from the antigen inlet, over the IDE arrays, and to the outlet. The antibody solution was introduced into the sensing electrodes using the antibody inlets and was immobilized on the sensing electrode array. After the test solution filled the microchannel, the flow was stopped for 30 minutes in order to facilitate efficient binding between *E. coli* and the antibody. This results in the impedance changes. The unbound *E. coli* cells were washed away using DI water.

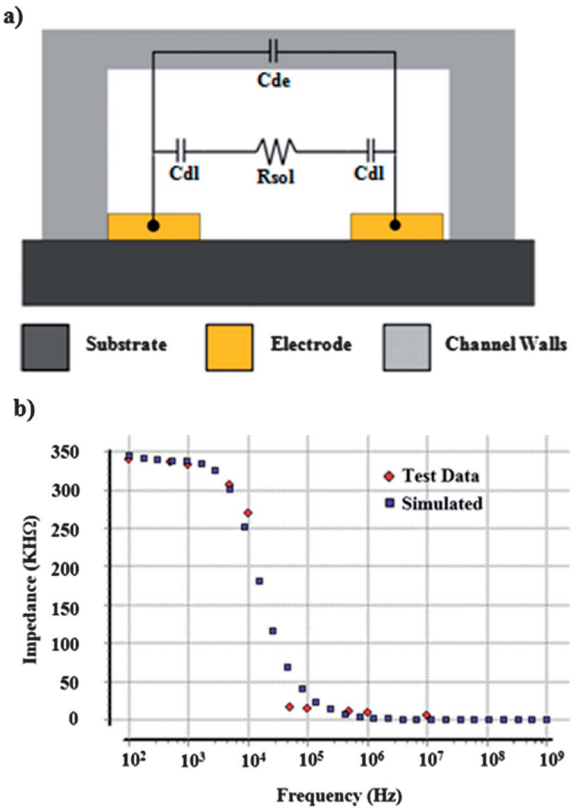

Fig. 2 (a) Equivalent circuit of the impedance biosensor demonstrating various circuit components. (b) Impedance spectrum demonstrating test data and simulated spectrum.

Electrical equivalent circuit

To study the impedance response, the equivalent electrical circuit of the biosensor was analysed. Fig. 2a represents an equivalent circuit of the impedance biosensor, which consists of two double layer capacitances (C_{dl}) in series with the bulk solution resistance (R_{sol}) and parallel to dielectric capacitance (C_{de}) of the system. Test solution present between the electrodes contributes towards the resistive component in the equivalent circuit. This is represented as resistance of the solution (R_{sol}). When two electrode surfaces are separated and have an

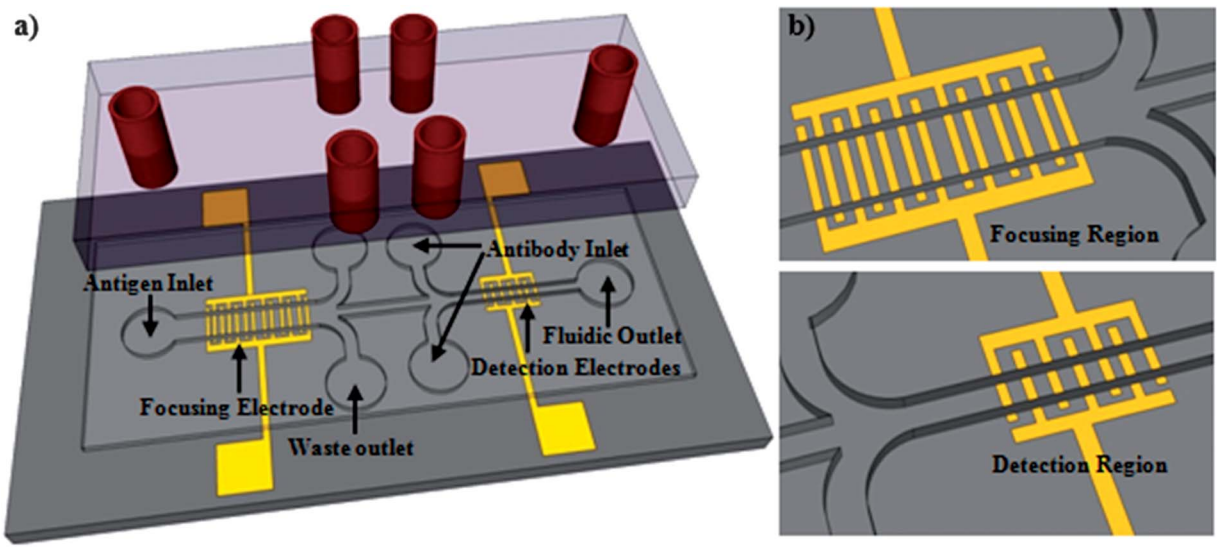

Fig. 1 3-D schematic of (a) the impedance based biosensor for pathogens detection. (b) Magnified view of the focusing region, and detection region.

electrolyte between them, a thin layer of charged particles form on the surface of the electrodes.

This layer of charged particles generates capacitance, known as double layer capacitance (C_{dl}). The dielectric capacitance (C_{de}) represents the overall capacitance of the dielectric medium.

Fig. 2b demonstrates experimental and simulated data (Bode plot) for the electrical equivalent circuit. EIS spectrum analyser software was used to simulate the response of the equivalent circuit and generate the fitting impedance spectrum. The simulation values of C_{dl} value vary from 50 nF to 97 nF, whereas R_{sol} values range from 305k to 340k depending on the bacterial concentration of the test sample. There are three distinctive regions in the impedance spectrum, which represents the response of the various components of the equivalent circuit individually and in combination. At low frequencies (100 Hz–1 KHz) the impedance response is dominated by capacitive impedance (mainly C_{dl}).The 1 KHz–10 KHz region of the impedance spectrum is due to the response of the both resistive and capacitive components and the response becomes purely resistive above 50 KHz frequencies. This is because; at low frequencies impedance of a capacitive effect dominates and nears zero at high frequencies. Hence the impedance response at high frequencies is solely due to the resistive component of the solution and the effect of bacterial cells is insignificant. In contrast, at lower frequencies the impedance response is significantly affected by the amount of bacteria present in the test solution. Thus, impedance measurement was performed in the range of 100 Hz to 1 MHz to obtain a viable Bode plot.

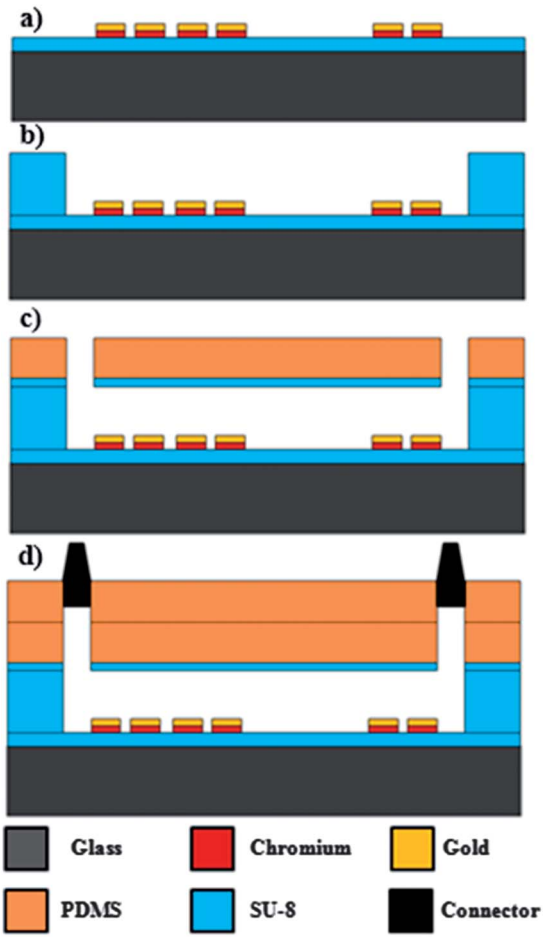

Fig. 3 Cross-sectional profile of the biosensor demonstrating various steps during the fabrication process of the MEMS impedance biosensor.

Microfabrication

The device was fabricated on a glass substrate using a series of surface micromachining, SU-8 photoresist and PDMS processes (Fig. 3). (1) The glass slides were cleaned using a piranha solution in 3 : 1 ratio of sulfuric acid and hydrogen peroxide ($H_2SO_4 : H_2O_2$) for 3 min in order to remove the organic contaminants from the substrate surface, then washed thoroughly with DI water and dried with a nitrogen blower. (2) Immediately after the cleaning, a layer of SU-8 photoresist (Microchem 2005) with approximate thickness of 4 μm was spin coated onto the glass slides. This was followed by a UV flood exposure without masking. The substrate was then hard baked at 150 °C for 30 min to cure the SU-8 layer. This additional layer of SU-8 improved the adhesion between the following SU-8 (Microchem 2005) channel and glass substrate, preventing it from peeling off from the substrate. (3) Two layers of titanium (Ti) and gold (Au) were deposited, using magnetron RF sputtering at 4 mTorr, with a thickness of 30 nm and 150 nm, respectively. Gold film was patterned using wet etching in potassium iodide (KI) and iodine (I_2) mixture, and Cr was etched using ready Cr etchant in order to create the IDE arrays, the electrode traces and bonding pads (see Fig. 3a). (4) The microchannel was defined using SU-8 (Microchem 2025) with a thickness of 25 μm (Fig. 3b). The SU-8 microchannel was then treated to improve its biocompatibility. It was first UV exposed at 450 mJ cm^{-2} for 1 hour and then oven baked at 150 °C for 24 hours. It was finally exposed to oxygen plasma for 20 seconds and Isopropanol (IPA) wash for 1 minute. (5) Two polydimethylsiloxane (PDMS) slabs were made and cured to serve as top cover along with fluidic connectors (fluidic inlets and outlets). (6) An oxygen plasma treatment was applied on the first PDMS slab, which has openings for inlet and outlet, in order to change its surface to hydrophilic and then SU-8 was spin coated onto it and cured at 95 °C for 10 minute for better adhesion.

The oxygen plasma step was used to improve the adhesion of SU-8 to PDMS. (7) The microchannel was then aligned and bonded to the PDMS/SU-8 cover manually and baked on a hotplate at 48 °C for 1 hour while pressure was applied to secure the bonding. The PDMS/SU-8 cover and SU-8 microchannel were cross-linked and formed a strong bond (Fig. 3c). (8) The second PDMS slab was prepared and cured along with the fluidics connector. It was then exposed to oxygen plasma, aligned manually with the first PDMS layer and bonded (Fig. 3d). The fluidic connectors were further sealed using epoxy glue in order to improve the device reliability and eliminate any possible fluid leakage. Optical images and magnified view of the fabricated device along with a complete device with wire bonding, packaging and soldering for external connections are shown in Fig. 4.

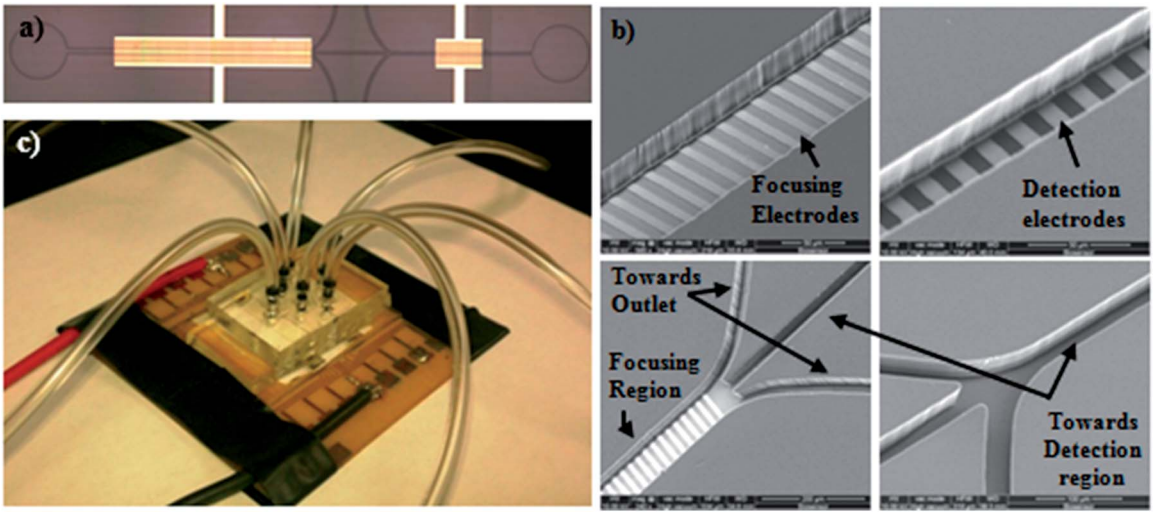

Fig. 4 Optical images and SEM micrographs of the fabricated impedance biosensor: (a) optical image of the fabricated device, (b) SEMs of the focusing and sensing IDE arrays along with the microfluidic channel, (left) is the focusing region, (right) is the detection region, (c) fabricated and packaged device.

Sample preparation

Preparation of *E. coli* and antibody samples. The *E. coli* broth was prepared by suspending 33 g mTSB broth with novobiocin powder (Sigma-Aldrich) into 1000 mL of distilled water. The solution was autoclaved at 121 °C for 15 minutes. The broth was inoculated with the *E. coli* O157:H7 (ATCC) that was grown on a previously cultured plate obtained using an inoculating loop (Fisher Scientific). The culture broth was then incubated for about 24 hours before it was used. The *E. coli* was cultured over a period of time in our lab, using Macconkey Sorbitol Agar (Remel Inc). The goat anti-*E. coli* O157:H7 antibody (Biodesign International) was diluted to a concentration of 50 μg mL^{-1} in Phosphate Buffer Saline (PBS) solution. The bacteria cultured broth measuring 3 mL was centrifuged (Horizon 642VES, Drucker Company) at 3200 rpm for 10 minutes. After the centrifugation, the supernatant was removed and the cells were re-dispersed in 3 mL PBS. The re-dispersed cells were centrifuged at 3200 rpm for 10 minutes and the step was repeated. The concentration of final purified cell suspension was approximately 2.5×10^5 CFU mL^{-1}. After the centrifugation was complete, the supernatant was removed and the cells were re-dispersed in 500 μl PBS solution. The total sample preparation time was less than an hour.

Immobilization

Goat anti-*E. coli* IgG antibodies were diluted to a concentration of 50 μg mL^{-1} in PBS solution. This antibody concentration was determined as the lowest concentration that produced a maximum impedance change, and showed the highest surface coverage, minimizing any subsequent nonspecific adsorption.[46] The antibody solution introduced from the inlets was immobilized on the IDE array for 30 minutes, during which the antibody was allowed to adsorb non-specifically onto the gold electrode surface. The media was then pumped out, and any unbound antibodies were washed using DI water. Next, *E. coli* samples were injected through inlet 1 over the immobilized antibodies. The immobilized *E. coli* binds to the antibody. Any unbounded *E. coli* were washed away using DI water, leaving the securely bonded antigen–antibody on the IDE array (Fig. 5).

Antigen labelling

The cells were purified at a concentration of 10^5 CFU mL^{-1} by centrifuging 5 mL contaminated soy broth at 3500 rpm for 10 min and then re-dispersed in 1 mL PBS. The cells were then exposed to 1.00 mM fluorescein isothiocyanate (FITC) in 1.00 mM sodium bicarbonate. The mixture was incubated for 1 h at room temperature in the dark. Next, the cells were centrifuged again to purify them from the free FITC. These cells were re-dispersed in 1 mL PBS solution, and used in the cell focusing experiment.[46]

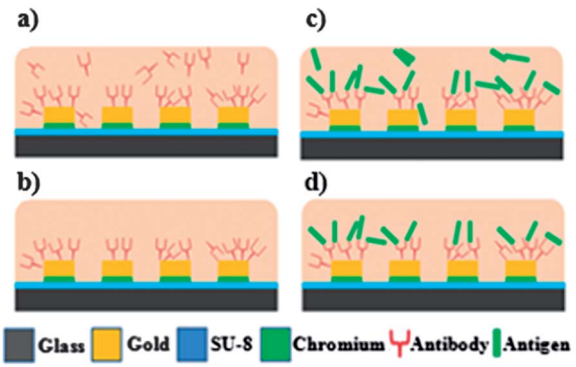

Fig. 5 Surface modification of the biosensor using polyclonal anti-*E. coli* antibody, and immobilization of *E. coli* to establish antibody–antigen binding. (a) Gold electrodes during antibody incubation period, (b) immobilized antibody on the electrode surface, (c) *E. coli* O157:H7 introduced on the modified electrodes' surface, (d) *E. coli* O157:H7 bound to the antibodies.

Results and discussions

Experimental setup

The experimental setup for characterizing the fabricated impedance biosensor is shown in Fig. 6. A syringe pump (a Harvard Apparatus PHD 2000) was used to inject fluid at different volumetric flow rates. A CCD camera installed on an inverted microscope was used to capture optical images of the device during experiment. An impedance analyzer (Agilent 4294A) was used to measure the impedance across the detection electrode array. The impedance was measured by applying an AC voltage of 0.5 V (peak-to-peak voltage) across the detection electrode array. The corresponding impedance values were measured for frequencies between 100 Hz and 10 MHz. A function generator was used to apply AC voltage at various frequencies at the focusing IDE array in order to generate p-DEP and optimize the focusing capability of the device.

Focusing effect

To study the focusing effect, the biosensor was first tested using polystyrene microbeads which have similar electrical properties to cells and were used to demonstrate the working principle of the process. Experimentally, we determined the amplitude and frequency of the applied signal that would generate positive dielectrophoresis (p-DEP) effects. Polystyrene microbeads with nominal diameter 10 μm in DI water were delivered from the inlet, and then focused in the center of the channel when an AC E-field (5 V peak-to-peak at 5.6 MHz) was applied across the focusing electrodes (Fig. 6c). Optical images of the focusing effect are shown in Fig. 7.

Similar behaviour is demonstrated by biological cells too. Positive DEP forces attract the cells towards the electrode array and a very small flow rate of 2–4 μL per minute was used to selectively roll the cells through the center channel towards the detection electrode array. The combination of p-DEP and fluidic drag force is referred to as the "focusing effect" in this article. This process results in significant increase in the number of cells in the detection region. Optical images of the process are shown in Fig. 8. Fluorescently labelled cells were captured using p-DEP and then slowly released with adequate flow to achieve the focusing effect.

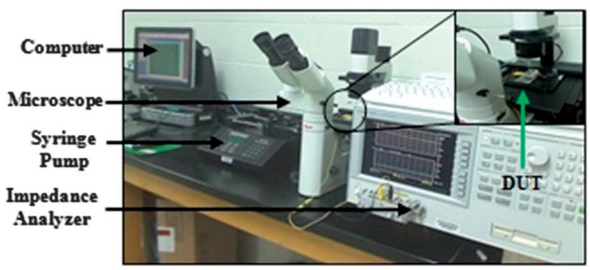

Fig. 6 An optical image of the biosensor test setup. The device under test (DUT) was placed on an inverted microscope with its inlets and outlets connected to a syringe pump and reservoirs, respectively. Electrical connections were made to the impedance analyzer and the computer for data acquisition. The function generator was used to deliver the required AC signal for p-DEP.

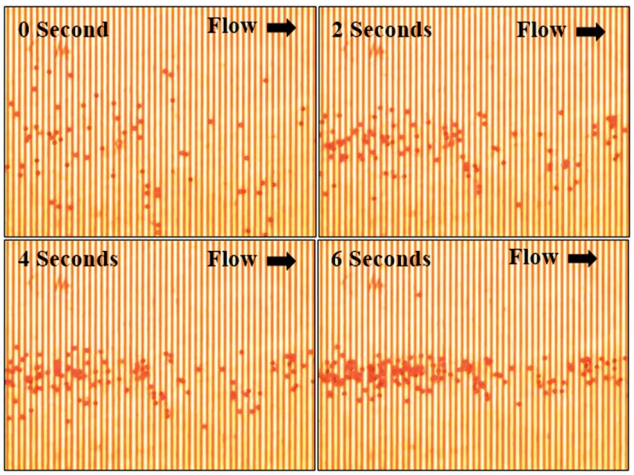

Fig. 7 Four sequential optical images recorded at various time intervals demonstrate the focusing effect on the microbeads.

Impedance response without focusing effect

Four serial concentrations of *E. coli* samples (3×10^5 CFU mL^{-1} to 3×10^2 CFU mL^{-1}) were tested. Initially, the impedance of the detection IDE array was measured in DI water using Agilent 4294A impedance analyzer over a frequency range of 100 Hz–10 MHz. The bare electrode array's impedance value was later used to confirm the adsorption of the antibody on the gold electrode surface. The anti-*E.coli* IgG antibodies (Ab) were pumped on to the detection electrode microchannel *via* the antibody inlets. These were non-specifically adsorbed on the electrode surface to ensure selective detection of *E.coli* cells. As the antibodies were adsorbed, the impedance of the electrode array increased. This increase in impedance demonstrates that the antibodies successfully adsorbed on the electrode surface. The measured antibody impedance was used as the baseline impedance in order to accurately determine the *E. coli* impedance. In the first experiment *E. coli* samples were tested without applying any DEP force. The cells were immobilized on the antibody coated detection electrodes for 30 minutes to successfully bind to the antibody. The antigen–antibody binding resulted in increased impedance. This was expected because the sensing electrode surface was modified for selective binding of *E. coli* O157:H7 cells with the antibody. The results demonstrate that the biosensor was able to detect the *E. coli* cells, with the lower detection limit being 3×10^2 CFU mL^{-1}. Fig. 8a shows the impedance spectra of the bonded *E. coli* cells which is calculated by subtracting the baseline impedance (antibody impedance) from the *E. coli*-antibody impedance. Each experiment was repeated 9 times and obtained results were compared to traditional cell counting methods to ensure reproducibility and reliability of the data. The time required for impedance detection without any focusing effect is about 45 minutes (Fig. 9).

Impedance response with focusing effect

In the next stage, the impedance response of *E. coli* was measured at the detection electrode with the focusing effect on

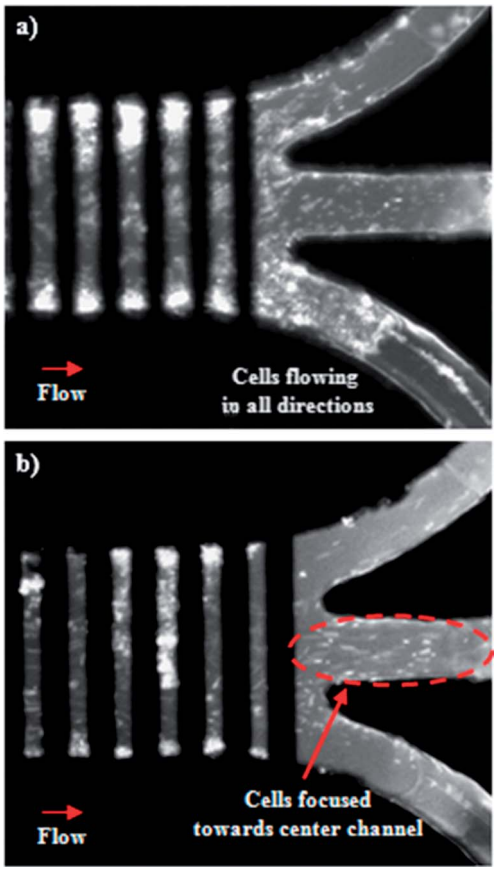

Fig. 8 Optical images of the fluorescently labeled cells in the focusing electrode region. (a) With, and (b) without "focusing effect".

the focusing electrode array IDE array and detection IDE array. Fig. 9b shows the impedance spectra of the *E. coli* samples of various concentrations which were recorded with focusing effect in play. The detection IDE array response showed that the measured impedance was directly proportional to the concentration of bacteria bound to the antibody on the electrode surface, and it was a significantly higher (1.7 to 2.2 times) than the impedance value obtained without the focusing effect. From the obtained result it can be inferred that, as focusing effect increases the number of target cells per unit volume in the detection region, there is an improvement in the signal level.

Impedance response with focusing effect and secondary DEP

To further improve the signal level, in conjunction with focusing effect, a secondary p-DEP force was applied on the detection electrode array. As noted earlier, p-DEP force attracted the cells towards the electrode surface, which result in increased antibody–antigen binding. This was also noted in the measured impedance spectrum for different concentrations. The impedance values increased notably, demonstrating improved capturing of *E. coli* cells on the detection IDE array, and hence increased measurement sensitivity. The impedance response of the biosensor after the applying p-DEP is shown in Fig. 9c.

A comparison of the three experiment values at 1 kHz was plotted as a function of *E. coli* concentration in Fig. 9d. The results clearly indicate that the use of focusing effect on the first IDE array significantly increased the measurement sensitivity. In addition, the p-DEP force on the detection IDE array further enhanced the measurement sensitivity. Hence, the use of p-DEP on both the electrodes in conjunction with impedance spectroscopy, have demonstrated superior sensitivity and lower detection levels as compared with traditional impedance detection platforms. Total time required for impedance detection with focusing effect and secondary DEP is about 2 hours.

Analysis of impedance spectrum

From analysis of the obtained impedance spectra, it was noted that the impedance values at higher frequencies above 50 KHz were negligible and were independent of the bacteria concentration. This is in agreement with the analysis of the equivalent circuit assumption. The immobilized bacteria also do not have any impact on the impedance values at high frequencies, as the impedance becomes purely resistive at such high frequencies. The impedance values at these high frequencies are believed to be the value of small dipole like bubbles and the resistance of the liquid medium. On the contrary, at lower frequencies the impedance response is mainly dependant on the double layer capacitance. This result obtained from the impedance spectrum implies that the amount of bacteria attached to the electrode surface can be correlated to the double-layer capacitance (C_{dl}) of the system. C_{dl} can be defined by the following equation.

$$C_{dl} = \varepsilon\varepsilon_0 \frac{A}{d}$$

ε and ε_0 are the dielectric constant of the electrolyte and the permittivity of free space respectively. A refers to the electrode area exposed to the electrolyte and d is the thickness of the double layer. From the above equation we see that, double-layer capacitance would be mainly dependent on the electrode area exposed. When bacteria cells immobilize on the electrode surface it effectively reduces the electrode area exposed to the electrolyte. Therefore, the decrease in the double-layer capacitance is thought to predominantly come from attached bacteria and bacteria-associated materials. As more bacteria attaches to the surface the exposed electrode area shrinks, which obstructs the double-layer charging. Reduced double layer capacitance increases the overall impedance of the system. Hence, the impedance values are higher at lower frequencies for higher concentration samples and lower for samples with low bacterial concentration. Thus it can be inferred that, the impedance response of the biosensor is dependent on both frequency and bacterial concentration.

Specificity testing

The biosensor was tested with a serotype of *E. coli* O104:H4 cells in order to confirm its specificity. The measured response showed no significant difference in impedance value with respect to the base impedance of the IDE array. This was to be

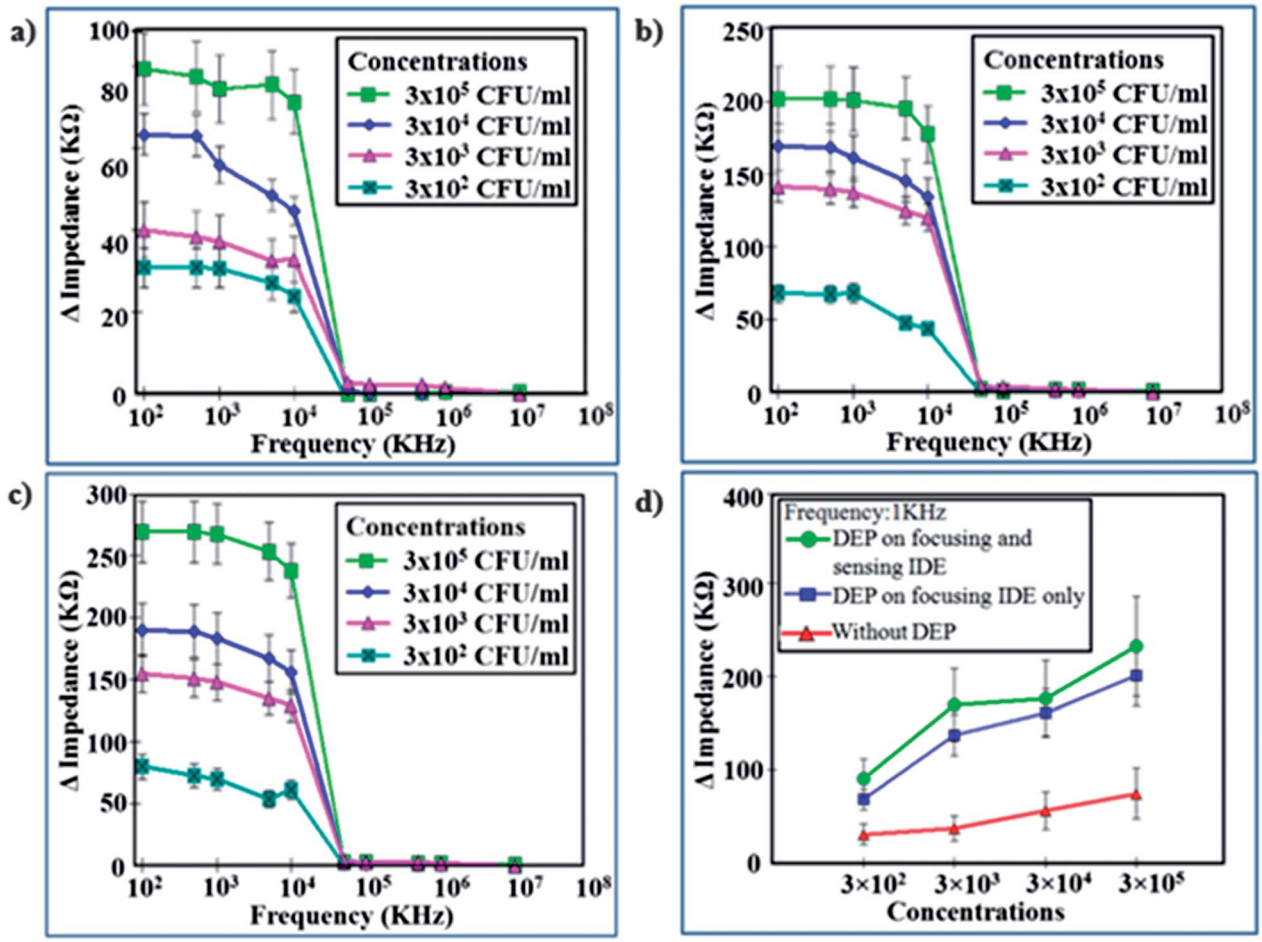

Fig. 9 Impedance response of the biosensor for (a) without focusing effect (b) with focusing effect and (c) with focusing effect in conjunction with applied p-DEP force at detection electrode array. (d) Comparison of impedance response at 1 KHz for samples with various concentration before and after applying p-DEP on the focusing electrode, and after applying p-DEP on both focusing and detection IDE arrays.

expected as the sensing electrode surface was modified specifically using anti-*E. coli* O157:H7 antibody. Although some *E. coli* O104:H4 cells may have non-specifically attached to the electrode surface, their numbers were so insignificant that it didn't produce enough change in the impedance value. This also suggests that, good antibody coverage of the electrode's surface was obtained and the anti-*E. coli* antibody doesn't attach to the non-*E. coli* O157:H7 cells. This demonstrates the specificity of the impedance biosensor in the presence of non-target bacterial cells.

Conclusion

In this study, we established a micromachined impedance biosensor platform with unique functionalities, in terms of its ability to use antibody–antigen recognition, dielectrophoretic cell focusing and impedance spectroscopy to achieve accurate low level bacteria detection capability within 3 hours. The polyclonal anti-*E. coli* antibody coated sensing IDE array ensures specific detection of *E. coli* O157:H7 bacterial cells. The biosensor was able to successfully detect *E. coli* concentrations up to 3×10^2 CFU mL^{-1}, The device was tested between 100 Hz and 1 MHz frequency and the results show that the p-DEP increases the measurement sensitivity by a factor of 2.9 to 4.5 times depending on the bacterial concentration. The total required time for sample processing and detection was under 3 hours. This is significantly lower than traditional laboratory methods. The dielectrophoretic manipulation of the cells enabled us to concentrate the bacteria on top of sensing IDE array, which improves the overall performance of the device, compared to the conventional methods, that relies on the diffusion of the bacteria to the surface of the electrode.

Acknowledgements

This research is supported by National Science Foundation Grant no. ECCS-0925612.

References

1 http://www.cdc.gov/foodborneburden/, 2012.
2 http://www.cdc.gov/outbreaknet/outbreaks.html, 2012.
3 http://www.cdc.gov/salmonella/outbreaks.html, 2012.

4 R. L. Scharff, Economic Burden from Health Losses Due to Foodborne Illness in the United States, *J. Food Prot.*, 2012, **75**(1), 123–131.
5 S. S. Park, R. W. Worobo and R. A. Durst, *Escherichia coli* O157: H7 as an emerging foodborne pathogen: a literature review, *Crit. Rev. Biotechnol.*, 2001, **21**, 27–48.
6 C. Murphy, C. Carroll and K. N. Jordan, Environmental survival mechanisms of the foodborne pathogen *Campylobacter jejuni*, *J. Appl. Microbiol.*, 2006, **100**, 623–632.
7 V. Velusamy, K. Arshak, O. Korostynska, K. Oliwa and C. Adley, An overview of foodborne pathogen detection: in the perspective of biosensors, *Biotechnol. Adv.*, 2010, **28**, 232–254.
8 R. L. Buchanan and M. P. Doyle, Foodborne disease significance of *Escherichia coli* O157:H7 and other enterohemorrhagic *E. coli*, *Food Technol.*, 1997, **51**(10), 69–76.
9 L. Yang and R. Bashir, Electrical/electrochemical impedance for rapid detection of foodborne pathogenic bacteria, *Biotechnol. Adv.*, 2008, **26**, 135–150.
10 L. P. Mansfield and S. J. Forsythe, The detection of *Salmonella serovars* from animal feed and raw chicken using a combined immunomagnetic separation and ELISA method, *Food Microbiol.*, 2001, **18**(4), 361–366.
11 W. Chen, G. Martinez. and A. Mulchandani, Molecular beacons: a real-time polymerase chain reaction assay for detecting Salmonella, *Anal. Biochem.*, 2000, **280**(2), 166–172.
12 C. L. Jacovides, R. Kreft, B. S. Bahar Adeli, B. Hozack, G. D. Ehrlich and J. Parvizi, Successful Identification of Pathogens by Polymerase Chain Reaction (PCR)-Based Electron Spray Ionization Time-of-Flight Mass Spectrometry (ESI-TOF-MS) in Culture-Negative Periprosthetic Joint Infection, *J. Bone Jt. Surg.*, 2012, **94**(24), 2247–2254.
13 H. P. Dwivedi and L. A. Jaykus, Detection of pathogens in foods: the current state-of-the-art and future directions, *Crit. Rev. Microbiol.*, 2011, **37**(1), 40–63.
14 J. J. Yu, L. D. Xiao and M. Yang, A PDMS microfluidic chip with nanostructures for bacteria concentration and fast detection, *IEEE MEMS 2008 Conference*, 2008, pp. 272–275.
15 A. D. Taylor, J. Ladd, Q. Yu, S. Chen, J. Homola and S. Jiang, Quantitative and simultaneous detection of four foodborne bacterial pathogens with a multi-channel SPR sensor, *Biosens. Bioelectron.*, 2006, **22**, 752–758.
16 X. Su and Y. Li, A self-assembled monolayer-based piezoelectric immunosensor for rapid detection of *Escherichia coli* O157:H7, *Biosens. Bioelectron.*, 2004, **19**(6), 563–574.
17 S. Sengupta, D. A. Battigelli and H.-C. Chang, A micro-scale multi-frequency reactance measurement technique to detect bacterial growth at low bio-particle concentrations, *Lab Chip*, 2006, **5**, 682–692.
18 R. Gomez, D. T. Morisette and R. Bashir, Impedance microbiology-on-a-chip: microfluidic bioprocessor for rapid detection of bacterial metabolism, *J. Microelectromech. Syst.*, 2005, **14**, 829–838.
19 Á. Rios, M. Zougaghb and M. Avila, Miniaturization through lab-on-a-chip: utopia or reality for routine laboratories? A review, *Anal. Chim. Acta*, 2012, **740**, 1–11.
20 L. Lu, G. Chee, K. Yamada and S. Jun, Electrochemical impedance spectroscopic technique with a functionalized microwire sensor for rapid detection of foodborne pathogens, *Biosens. Bioelectron.*, 2013, **42**, 492–495.
21 M. S. Mannoor, S. Zhang, A. J. Link and M. C. McAlpine, Electrical detection of pathogenic bacteria *via* immobilized antimicrobial peptides, *Proc. Natl. Acad. Sci. U. S. A.*, 2010, **107**(45), 19207–19212.
22 R. L. Caygill, G. E. Blair and P. A. Millner, A review on viral biosensors to detect human pathogens, *Anal. Chim. Acta*, 2010, **681**(1–2), 8–15.
23 M. Díaz-Serrano, A. Rosado, J. delPilar, M. Arias and A. R. Guadalupe, A Polymer-Based Electrochemical DNA Biosensor for Salmonella: Preparation, Characterization and Calibration, *Electroanalysis*, 2011, **23**(8), 1830–1841.
24 S. Siddiqui, Z. Dai, C. J. Stavis, H. Zeng, N. Moldovan, R. J. Hamers, J. A. Carlisle and P. U. Arumugam, A quantitative study of detection mechanism of a label-free impedance biosensor using ultrananocrystalline diamond microelectrode array, *Biosens. Bioelectron.*, 2012, **35**(1), 284–290.
25 V. K. K. Upadhyayula, Functionalized gold nanoparticle supported sensory mechanisms applied in detection of chemical and biological threat agents: a review, *Anal. Chim. Acta*, 2012, **715**, 1–18.
26 B. S. Ferguson, S. F. Buchsbaum, T.-T. Wu, K. Hsieh, Y. Xiao, R. Sun and H. T. Soh, Genetic analysis of H1N1 influenza virus from throat swab samples in a microfluidic system for point-of-care diagnostics, *J. Am. Chem. Soc.*, 2011, **133**(23), 9129–9135.
27 Y. Yin, M. M. M. Bilek, K. Fisher, C. Guo and D. McKenzie, An integrated solution for rapid biosensing with robust linker free covalent binding surfaces, *Biosens. Bioelectron.*, 2013, **42**(1), 447–452.
28 T. F. McGrath, K. Andersson, K. Campbell, T. L. Fodey and C. T. Elliott, Development of a rapid low cost fluorescent biosensor for the detection of food contaminants, *Biosens. Bioelectron.*, 2013, **41**(1), 96–102.
29 P. Arora, A. Sindhu, H. Kaur, N. Dilbaghi and A. Chaudhury, An overview of transducers as platform for the rapid detection of foodborne pathogens, *Appl. Microbiol. Biotechnol.*, 2013, 1–12.
30 A. Henseleit, S. Schmieder, T. Bley, F. Sonntag, N. Schilling, P. Quenzel, N. Danz, U. Klotzbach and E. Boschke, A compact and rapid aptasensor platform based on surface plasmon resonance, *Eng. Life Sci.*, 2011, **11**(6), 573–579.
31 W.-K. Oh, Y. S. Jeong, J. Song and J. Jang, Fluorescent europium-modified polymer nanoparticles for rapid and sensitive anthrax sensors, *Biosens. Bioelectron.*, 2011, **29**(1), 172–177.
32 T. Q. Huy, N. T. H. Hanh, N. T. Thuy, P. V. Chung, P. T. Nga and M. A. Tuan, A novel biosensor based on serum antibody immobilization for rapid detection of viral antigens, *Talanta*, 2011, **86**(1), 271–277.

33 H.-J. Lee, J.-H. Lee and H.-I. Jung, A symmetric metamaterial element-based RF biosensor for rapid and label-free detection, *Appl. Phys. Lett.*, 2011, **99**(16), 163703.

34 D. Zhang, D. J. Carr and E. C. Alocilja, Fluorescent bio-barcode DNA assay for the detection of *Salmonella enteric* serovar enteritidis, *Biosens. Bioelectron.*, 2009, **24**(5), 1377–1381.

35 B. N. Johnson and R. Mutharasan, Biosensing using dynamic-mode cantilever sensors: a review, *Biosens. Bioelectron.*, 2012, **32**(1), 1–18.

36 V. Chan, J. H. Jeong, P. Bajaj, M. Collens, T. Saif, H. Kong and R. Bashir, Multi-material bio-fabrication of hydrogel cantilevers and actuators with stereolithography, *Lab Chip*, 2012, **12**(1), 88–98.

37 K. Gruber, T. Horlacher, R. Castelli, A. Mader, P. H. Seeberger and B. A. Hermann, Cantilever array sensors detect specific carbohydrate–protein interactions with picomolar sensitivity, *ACS Nano*, 2011, **5**(5), 3670–3678.

38 K. Narsaiah, S. N. Jha, R. Bhardwaj, R. Sharma and R. Kumar, Optical biosensors for food quality and safety assurance-a review, *J. Food Sci. Technol.*, 2012, **49**(4), 383–406.

39 R. Amin, A. Kulkarni, T. Kim and S. H. Park, DNA thin film coated optical fiber biosensor, *Curr. Appl. Phys.*, 2012, **12**(3), 841–845.

40 T. R. J. Holford, F. Davis and S. P. J. Higson, Recent trends in antibody based sensors, *Biosens. Bioelectron.*, 2012, **34**(1), 12–24.

41 R. Bharadwaj, V. V. R. Sai, K. Thakare, A. Dhawangale, T. Kundu, S. Titus, P. K. Verma and S. Mukherji, Evanescent wave absorbance based fiber optic biosensor for label-free detection of *E. coli* at 280nm wavelength, *Biosens. Bioelectron.*, 2011, **26**(7), 3367–3370.

42 X. Guo, C.-S. Lin, S.-H. Chen, R. Ye and V. C. H. Wu, A piezoelectric immunosensor for specific capture and enrichment of viable pathogens by quartz crystal microbalance sensor, followed by detection with antibody-functionalized gold nanoparticles, *Biosens. Bioelectron.*, 2012, **38**(1), 177–183.

43 W. Pang, H. Zhao, E. S. Kim, H. Zhang, H. Yu and X. Hu, Piezoelectric microelectromechanical resonant sensors for chemical and biological detection, *Lab Chip*, 2012, **12**(1), 29–44.

44 C. Yu, J. Vykoukal, D. M. Vykoukal, J. A. Schwartz, L. Shi and R. C. Gascoyne, A Three-Dimensional Dielectrophoretic Particle Focusing Channel for Microcytometry Applications, *J. Microelectromech. Syst.*, 2005, **14**, 480–487.

45 B. Cetin, Y. Kang, Z. Wu and D. Li, Continuous particle separation by size *via* AC-dielectrophoresis using a lab-on-a-chip device with 3-D electrodes, *Electrophoresis*, 2009, **30**(5), 766–772.

46 M. Dweik, R. C. Stringer, S. Ghosh Dastider, Y. Wu, M. Almasri and S. Barizuddin, Specific and targeted detection of viable *Escherichia coli* O157:H7using a sensitive and reusable impedance biosensor with dose and time response studies, *Talanta*, 2012, **94**, 84–89.

